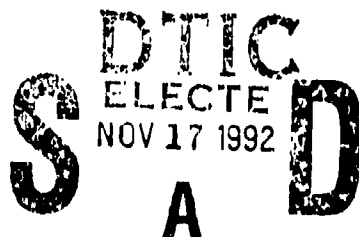AD-A257 348

ARMY RESEARCH LABORATORY

AR

The Velocity Difference Between Particulated Shaped Charge Jet Particles for Face-Centered-Cubic Liner Materials

William P. Walters
Richard L. Summers

ARL-TR-8   November 1992

DTIC
ELECTE
NOV 17 1992
S   D
A

92-29627

NOTICES

REPORT DOCUMENTATION PAGE

1. AGENCY USE ONLY (Leave blank)	2. REPORT DATE	3. REPORT TYPE AND DATES COVERED
	November 1992	Final, January 1991–June 1992

4. TITLE AND SUBTITLE

The Velocity Difference Between Particulated Shaped Charge Jet Particles for Face-Centered-Cubic Liner Materials

5. FUNDING NUMBERS

PR: 1L162618AH80

6. AUTHOR(S)

William P. Walter and Richard L. Summers

7. PERFORMING ORGANIZATION NAME(S) AND ADDRESS(ES)

U.S. Army Research Laboratory
ATTN: AMSRL-WT-TC
Aberdeen Proving Ground, MD 21005-5066

8. PERFORMING ORGANIZATION REPORT NUMBER

9. SPONSORING/MONITORING AGENCY NAME(S) AND ADDRESS(ES)

U.S. Army Research Laboratory
ATTN: AMSRL-OP-CI-B (Tech Lib)
Aberdeen Proving Ground, MD 21005-5066

10. SPONSORING/MONITORING AGENCY REPORT NUMBER

ARL-TR-8

11. SUPPLEMENTARY NOTES

12a. DISTRIBUTION/AVAILABILITY STATEMENT

Approved for public release; distribution is unlimited.

12b. DISTRIBUTION CODE

13. ABSTRACT (Maximum 200 words)

A model was derived to predict the average jet velocity difference between particulated shaped charge jet particles. The model is based on the "wire drawing" formula presented by Kolsky, the plastic instability criterion, and the Zerilli-Armstrong constitutive equation for face-centered-cubic materials. The velocity difference expression is strongly dependent on the jet temperature and weakly dependent on the jet strain rate. Calculations were also made using the Johnson-Cook constitutive model. The average velocity difference between jet particles, the true stress at necking, and the true strain at necking were calculated using several variants of the model. Velocity difference comparisons with experimental data were made for several shaped charge designs with copper liners of various geometries.

14. SUBJECT TERMS

shaped charges; jet characteristics; jet breakup time; velocity difference; jet particles; strain rate effects; strain rate

15. NUMBER OF PAGES

40

16. PRICE CODE

17. SECURITY CLASSIFICATION OF REPORT	18. SECURITY CLASSIFICATION OF THIS PAGE	19. SECURITY CLASSIFICATION OF ABSTRACT	20. LIMITATION OF ABSTRACT
UNCLASSIFIED	UNCLASSIFIED	UNCLASSIFIED	UL

INTENTIONALLY LEFT BLANK.

TABLE OF CONTENTS

Accesion For

NTIS   CRA&I
DTIC   TAB
Unannou...ed
Justification

By
Distribution /

Availability Codes

Dist   Avail a...or
        Special

A-1

III

INTENTIONALLY LEFT BLANK.

LIST OF FIGURES

INTENTIONALLY LEFT BLANK.

LIST OF TABLES

INTENTIONALLY LEFT BLANK.

1. INTRODUCTION

A shaped charge consists of a cylinder of explosive with a hollow cavity in one end and a detonator at the opposite end. The hollow cavity, which may assume almost any geometric shape such as a hemisphere, a cone, tulip, trumpet, or, in fact, any arcuate device is usually lined with a thin layer of metal. The liner forms a jet when the explosive charge is detonated. Upon initiation, a spherical wave propagates outward from the point of initiation. This high pressure shock wave moves at a very high velocity, typically around 8 km/s. As the detonation wave engulfs the lined cavity, the material is accelerated under the high detonation pressure, collapsing the liner. During this process, the liner material is driven to very violent distortions over very short time intervals, at strain rates of 10^4–10^7 s^{-1}. High strains are readily achieved since superimposed on the deformation are very large hydrodynamic pressures (peak pressures of approximately 200 GPa, decaying to an average of approximately 20 GPa). For conical liners, the collapse of the liner material onto the centerline forces a portion of the liner to flow in the form of a jet where the jet tip velocity can travel in excess of 10 km/s. The jet temperature is about 500–900 K according to the measurements of von Holle and Trimble (Walters and Zukas 1989) for a shaped charge with a copper conical liner. Also, there are undoubtedly temperature gradients along and through the jet. Because of the presence of an axial velocity gradient, the jet will stretch until it fractures into a column of particles. This fracture of the jet into a series of particles is termed jet breakup or particulation. Associated with the particulation of a shaped charge jet, there exists an average particle length of the particulated jet segments with an average velocity difference between them.

There are at least three reasons for attempting to calculate the velocity difference (ΔV) between particulated shaped charge jet particles. First, this ΔV is usually 0.1 km/s for most jets from copper conical liners. Thus, attempting to calculate a known (or approximately known) quantity may serve to verify the calculational and modeling method used to characterize the liner material and the particulation process. Second, the ΔV between particulated jet particles may be linked to the calculation of jet breakup time if $\Delta V = \Delta L/\tau$, where ΔV is the velocity difference between particulated jet particles, ΔL is the characteristic length or change in particle length which occurs over the interval ΔV, and τ is the average jet breakup time, measured from some reference point (when the detonation wave hits the liner,

1

from the initiation of the detonator, when the liner element in question arrives at the jet axis of symmetry, the virtual origin, etc.). Third, if the penetration of a particulated jet is calculated incrementally, i.e., particle by particle, then the separation distance and velocity between jet particles must be known.

The nature of the particulation of the shaped charge jet, and the associated average velocity difference between particles, has been of interest for over 50 years. It is known that certain liner materials exhibit extreme ductility under the intense dynamic conditions involved in the shaped charge collapse process. These materials often do not possess the same degree of ductility under ambient conditions and can undergo dynamic elongations of 1,000% or more. The problem is complicated by the fact that the material properties of the liner are not well known under the intense dynamic conditions that the jet undergoes during its collapse, formation, and growth. Complex hydrocode computer programs are limited because accurate equations of state and constitutive equations are not available under these conditions. Also, the fracture mechanism and associated algorithm is not well known. Nevertheless, shaped charge experiments provide an excellent test bed for the study of materials under intense loading conditions.

This report will address the analytical calculation of the ΔV between particulated jet particles. The calculation is dependent upon an appropriate constitutive equation. Three constitutive equations are examined—the Zerilli-Armstrong model for face-centered-cubic liner materials (notably copper), the Johnson-Cook, and the modified Johnson-Cook equations. Future studies will concern body-centered-cubic materials and the calculation of jet particulation (breakup) time.

1.1 Experimental Approach. The experimental characterization of shaped charge jets is most commonly performed using multiple flash x-ray units. Each flash x-ray unit provides an image of the shaped charge jet at a known time. In a typical experiment, several x-ray units are flashed at predetermined time intervals. In general, the entire shaped charge jet cannot be captured in a single experiment due to limitations in the length of x-ray film which can be exposed and the need to protect the film from the explosive blast. The x-ray films are analyzed to determine the position, length, radius, mass, and velocity of each of the jet particles. The velocity of a jet particle is determined from the position of the particle's center

2

of mass at each flash time (Summers and Wright 1992). Once the velocity of each jet particle has been derived, the calculation of the velocity difference between adjacent jet particles is trivial.

The velocity difference between particles for a jet from a copper liner typically ranges from nearly 0 to 250 m/s. The highest values of ΔV are observed between two particles which separate earlier than the neighboring particles. This variation in separation time and ΔV is attributed to inhomogeneities in the shaped charge jet material. The average ΔV between jet particles over all particles from a single jet is relatively constant, between 80 m/s and 130 m/s, for most copper jets regardless of the liner size or geometry.

1.2 Previous Analytical Models. Analytical models to estimate the ΔV between jet particles are available, notably due to Held, Carleone and Chou, Pfeffer, Haugstad, and Hirsch. These ΔV models are generally by-products of breakup time calculation models. All of the ΔV models are one-dimensional and primarily semiempirical.

Other studies which are related to jet breakup time but provide some insight into mechanisms behind jet particulation, jet ductility, and/or the velocity difference between particulated jet particles are given below. Shelton and Arbuckle (1979) considered the propagation of relief waves following a break in the jet. The speed of relief wave propagation from the break was calculated by two different models. Walsh (1984) provided insight into certain mechanisms, i.e., surface disturbances, that may lead to jet instability. These disturbances include explosive homogeneity, liner dimensional tolerance, velocity gradient perturbations, and liner dynamic strength variations. Walsh concluded that breakup depends on the perturbation structure and a single dimensionless flow parameter

$$\phi = \frac{\sigma}{\rho \Delta V_o^2 R},$$

where σ is the yield strength of the jet, ρ is its density, R is the jet radius, and ΔV_o^2 is the initial jet stretch rate. The subscript "o" represents initial jet conditions. Finally, it was shown that the length traveled until breakup occurred $L_b = L_b (L_o, \phi_o, \Psi_o)$, where L_o is the initial jet

3

length, ϕ_n is the initial value of ϕ, and Ψ_0 is the initial surface roughness. Haugstad (1983) and Haugstad and Dullum (1983) formulated two models for the jet breakup time by considering viscoplastic effects of $\sigma = \sigma_0 + \mu\dot{\epsilon}$, where μ has the form of a viscosity, σ is the yield stress, σ_0 is the quasistatic yield stress, and $\dot{\epsilon}$ is the strain rate.

In addition to a formula for the jet breakup time, they determined the ΔV between particulated jet particles to be

$$\Delta V = 0.87 \sqrt{\frac{\sigma}{\rho}} \ .$$

Hirsch (1979) attempted to express a term defined as the plastic velocity (sometimes interpreted to be the ΔV between particulated jet particles) to be

$$V_{pl} = \sqrt{\frac{\sigma}{\rho}} \ ,$$

where σ is the liner metal dynamic yield stress and ρ is the density of the liner material. Hirsch employed the Mott fragmentation model as mentioned by Chou, Sidhu, and Mortimer (1963) and provided a description of the breakup time model as arising from shear bands or

$$V_{pl} = \sqrt{\frac{d\sigma_m}{\rho}} \ ,$$

where $d\sigma_m$ represents the difference between the isothermal and adiabatic stress-vs.-strain characteristics of the metal at the point where the adiabatic stress becomes a maximum. Hirsch quotes strains of 1 to 2 at a strain rate of 10^5 s^{-1} for OFHC copper. These values of strain are considerably lower than those quoted by Chou and Carleone (1976). Hirsch (1981a) further qualified the plastic velocity by suggesting a breakup mechanism where holes

4

caused by a pile up of vacancies are formed at the metal surface and gradually increase until breaking it (i.e., breakup is caused by the formation of voids in the jet). Hirsch also predicted the existence of a strain rate threshold below which other mechanisms dominate the breakup process. Hirsch (1981b) states that even perfectly symmetrical and homogeneous shaped charge configurations have transverse velocity components in the jet. This means that the breakup process starts during the liner collapse, and the transverse velocity influences the jet breakup and the ΔV between particles. Hirsch (1990) relates the plastic velocity to the processes which affect the liner metallurgical state during the initial stages of jet formation. Hirsch shows how both the deformation energy heating the sliding shear bands during the localization process and the rate of the instability growing in the plastic flow during this process combine to determine the plastic velocity parameter. This velocity is shown to be related to both the velocity due to the plastic deformation and the component of the maximum slide velocity allowable to form shear bands in the elongation direction. Hirsch thus attempts to include the influence of the metallurgical structure of the liner on the breakup time and ΔV. In this study, small strains (less than one) are calculated.

Pfeffer (1980) obtained a jet breakup time formula that indicates that the breakup time is inversely proportional to the initial strain rate, weakly dependent on the initial jet radius, but independent of the liner material yield strength. Pfeffer assumed a formula for the shape of the broken jet segment and also gave an expression for the ΔV between jet segments as

$$\Delta V = 0.95 \sqrt{\frac{\sigma}{\rho}} ,$$

where σ is the jet yield strength and ρ is the jet density. These results are based on a curve fit of two-dimensional computer simulations. Held (1989), quoting earlier studies by Trinks, reported on calculations based on the kinetic energy of a continuous and particulated jet. This energy balance revealed the velocity difference between the upper and lower velocities of a jet section before particulation to be $\Delta v = \sqrt{24\varepsilon\sigma/\rho}$. From the Chou-Carleone analysis (Chou, Carleone, and Karpp 1974; Chou and Flis 1986; Chou and Carleone 1977a, 1977b), it can be shown that $\Delta V = 0.7 \sqrt{\sigma/\rho}$. Table 1 lists the analytical expressions for the ΔV models. Note that all formulas yield a dependence on $\sqrt{\sigma/\rho}$. Also, note that the calculated ΔV will be the same for all shaped charge liner geometries of the same material once the

5

Table 1. Analytical Equations for the Prediction of the Velocity Difference Between Particulated Jet Particles

ΔV Expressions	
Investigators	ΔV =
Haugstad (1983), Haugstad and Dullum (1983)	$0.87 \sqrt{\sigma/\rho}$
Pfeffer (1980)	$0.95 \sqrt{\sigma/\rho}$
Hirsch (1979)	$\sqrt{\sigma/\rho}$
Chou-Carleone (1977a)	$0.7 \sqrt{\sigma/\rho}$
Held (1989)[a]	$\sqrt{\dfrac{24 \varepsilon \sigma}{\rho}}$

[a] Here, / ⋅ is the velocity difference between the upper and lower velocities of a jet before breakup

assumed constant yield strength is established for the liner material. In most breakup time models, the average jet breakup time is also dependent on $\sqrt{\sigma/\rho}$ and hence ΔV.

Held (1985), Mostert and Koenig (1987), Golaski and Duffy (1987), Chokshi and Meyers (1990), and Hirsch (1992) among others comment on the influence of liner metallurgy on the jet ductility. Golaski and Duffy (1987) did not provide a ΔV formula, but showed a direct correlation between liner grain size and jet breakup time. Mostert and Koening (1987) stated that the jet from a shaped charge elongates to a strain well in excess of 10 before it particulates. They also noted that the micromechanical properties of the liner, as well as its purity, have an influence on the ductility of the jet, but these factors are not included in any existing models. Factors which are known to affect jet breakup time, and hence jet ductility, are given by Held (1989) and Walters and Zukas (1989).

2. THE ANALYTICAL MODEL

2.1 Definitions. For clarity, the expressions for the stress, strain, and strain rate used in this study to convert from one definition to the other are specified below. It is noted that the definition of strain (or stress) is not clearly specified in most of the analytical models previously published. The engineering strain is defined as $\varepsilon_e = \dfrac{\ell - \ell_o}{\ell_o} = \dfrac{\ell}{\ell_o} - 1$, and the true strain $\varepsilon = \ln \dfrac{\ell}{\ell_o}$, where ℓ is the final length of the jet and ℓ_o is the initial length.

Thus, $d\varepsilon_e = \dfrac{d\ell}{\ell_o}$ and $d\varepsilon = \dfrac{d\ell}{\ell} = -\dfrac{dA}{A}$ since $A_o\ell_o = A\ell$ by the conservation of mass equation for incompressible flow. Also,

$$\dot{\varepsilon}_o = \frac{\dot{\ell}}{\ell_o} \text{ and } \dot{\varepsilon} = \frac{\dot{\ell}}{\ell}.$$

Hence,

$$\dot{\varepsilon}_o = \dot{\varepsilon}(\varepsilon_e + 1),$$

$$\varepsilon = \ln(\varepsilon_e + 1), \text{ and}$$

$$\varepsilon_e = \exp \varepsilon - 1.$$

The force $F = \sigma A = \sigma_e A_o$, where A_o is the initial cross-sectional area of the jet and σ and σ_e represent the true and engineering stresses, respectively.

Since $\dot{\varepsilon} = \Delta U$, where ΔU is the velocity difference (assumed constant) which results in the imposed stretch or strain rate, i.e., the difference between the tip velocity and the tail velocity of the jet, then

$$\dot{\varepsilon} = \frac{\Delta U}{\ell} = \dot{\varepsilon}_0 \exp(-\varepsilon).$$

2.2 Constitutive Equations. The particulation process, and the resulting average velocity difference between particulated jet particles, must depend on the constitutive behavior of the material, i.e., the stress-strain-strain-rate interdependency. The constitutive relationships chosen for this study were the Zerilli-Armstrong and the Johnson-Cook models since the exact functional forms and the values of the coefficients used in the equations are available. The Zerilli-Armstrong (1987) constitutive equation for face-centered-cubic materials is

$$\sigma = C_0 + k\lambda^{-1/2} + C_2\varepsilon^{1/2}\exp(-C_3T + C_4T\ln\dot{\varepsilon}). \tag{1}$$

The stress σ is in MPa, the strain rate $\dot{\varepsilon}$ is in s^{-1}, and the temperature T is in K. For an OFHC copper jet, Zerilli-Armstrong give

k $=$ microstructural stress intensity $=$ 5.0 MPa $(mm)^{1/2}$
λ $=$ grain size $=$ 0.075 mm
$C_0 =$ 46.5 MPa
$C_2 =$ 890.0 MPa
$C_3 =$ 0.0028 K^{-1}
$C_4 =$ 0.000115 K^{-1}.

The Johnson-Cook (1983, 1985) constitutive equation was investigated due to its popularity in many hydrocodes. Johnson (1983) reports

$$\sigma = (A + B\varepsilon^n)(1 + C\ln\dot{\varepsilon})(1 - T^{*m}), \tag{2}$$

8

and

$$T^* = (T - T_{room})/(T_{melt} - T_{room}),$$

$$0 \le T^* \le 1,$$

where for OFHC copper,

$$T_{melt} = 1{,}356 \text{ K}, \ T_{room} = 293 \text{ K}, \ C = 0.025,$$
$$m = 1.09, \ n = 0.31, \ A = 90.0 \text{ MPa, and } B = 292.0 \text{ MPa.}$$

Note that in the system of units used in the above equations, the density, ρ, of copper is 8,960 kg/m^3.

In addition, the modified Johnson-Cook model was examined. The modified Johnson-Cook equation is

$$\sigma = (A + B\varepsilon^n)\dot{\varepsilon}^C(1 - T^{*m}), \qquad (3)$$

where, for OFHC copper, all constants have the same value as in the original Johnson-Cook model, but the functional form of the strain rate has been changed.

Any constitutive equation may be used in this analysis, assuming of course that the parameters used in the equation are available and do not introduce additional unknowns (such as the pressure for example).

The Zerilli-Armstrong and Johnson-Cook constitutive equations may be evaluated to provide the values of stress and strain at the onset of plastic instability, or necking. The critical strain at necking is determined by the plastic stability criteria which states that

$$(\sigma + \delta\sigma)(A + \delta A) \ge \sigma A$$

for stability.

9

Here, A is the cross-sectional area, δA is an incremental element of area, and $\delta\sigma$ is an incremental element of stress. Neglecting higher order terms, the plastic stability inequality yields

$$\frac{\delta\sigma}{\sigma} \geq -\frac{\delta A}{A}$$

or

$$\frac{d\sigma}{d\varepsilon} \geq \sigma, \tag{4}$$

where now the true stress and true strain are used. From Equation 4, the strain at the onset of plastic instability, i.e., necking is calculated where

$$\frac{d\sigma}{d\varepsilon} = \sigma,$$

and $\dfrac{d\sigma}{d\varepsilon}$ and σ are obtained from either Equation 1, Equation 2, Equation 3, or any other appropriate constitutive equation.

For the Zerilli-Armstrong model, differentiation of Equation 1 yields

$$\frac{d\sigma}{d\varepsilon} = C_2 \exp(-C_3 T)\, \dot{\varepsilon}^{C_4 T}\, \varepsilon^{-1/2} \left[\frac{1}{2} - C_4 T \varepsilon\right], \tag{5}$$

where the true stress, strain, and strain rate values are used. Since

$$\dot{\varepsilon}^{C_4 T} = \dot{\varepsilon}_0^{C_4 T} \exp(-C_4 T \varepsilon),$$

Equations 1 and 5 can be used to obtain the true strain at the onset of necking.

An identical procedure is employed for the Johnson-Cook model, Equation 2, and the modified Johnson-Cook model, Equation 3. Table 2 lists the strains and stresses at the onset of necking for both constitutive equations. The values given in Table 2 are for an 81-mm-diameter conical copper liner with a tip velocity of 7.68 km/s and a measured tail velocity (last particle of the jet visible at all x-ray flash times) of 2.13 km/s. The initial strain rate was calculated to be 67,957 s^{-1}. The temperature was assumed to be 625 K, which is near the median range of the measured values from von Holle and Trimble reported in Walters and Zukas (1989). The copper grain size was taken to be 0.075 mm from Zerilli-Armstrong (1987).

The initial strain rate, $\dot{\varepsilon}_0$ is taken to be the difference in velocity between the fastest and the slowest jet particles divided by the effective slant height of the conical liner or the effective slant length (the perimeter of one-half of the inside surface) for a nonconical liner. Note that a part of the apex region for a conical liner contributes only to the mass of the tip, and a portion of the base region of the liner does not contribute to the jet. In general, the effective slant height is given by $\ell_0(V_{tip} - V_{rear})/V_{tip}$, where V_{tip} is the jet tip velocity, V_{rear} is the measured tail velocity from the flash x-ray of the jet (which depends on the length of jet captured on the film), and ℓ_0 is the total slant length of the liner. Thus,

$$\dot{\varepsilon}_0 = \frac{V_{tip}}{\ell_0} .$$

The ratio $(V_{tip} - V_{rear})/V_{tip}$ is introduced to account for the fact that the flash radiograph does not provide information on the entire length of the shaped charge jet. The effective slant height is intended to represent the portion of the shaped charge liner which is characterized in the jet free flight. However, as will be shown shortly, ΔV calculations are relatively insensitive to the initial strain rate.

The calculated strain values at necking from the Zerilli-Armstrong model are lower than the values quoted by Chou and Carleone (1976) or Mostert and Koenig (1987), and of the same order as those quoted by Hirsch (1990). The strains at necking calculated via the Johnson-Cook models are lower yet. However, for all constitutive equations, the true stress

11

Table 2. Stress and Strain Values at the Onset of Necking for the Zerilli-Armstrong and Johnson-Cook Constitutive Equations

	Zerilli-Armstrong	Johnson-Cook	Modified Johnson-Cook
ε	0.359	0.202	0.201
σ (MPa)	265.6	244.8	252.4
ε_θ	0.432	0.224	0.223
σ_θ (MPa)	185.5	200.0	206.4

values fall in the range of 100 to 300 MPa as quoted by most investigators. It is not obvious whether true or engineering stresses/strains are obtained by other investigators.

Also, the strain at necking predicted by the Zerilli-Armstrong constitutive equation increases with decreasing temperature. Therefore, jet breakup times that increase with decreasing temperature would be expected. This effect is due to the functional form of the Zerilli-Armstrong equation and not the ΔV model. The Johnson-Cook strains at necking do not vary with temperature and lead to the prediction of extremely low ΔV values. Figure 1 compares the calculated true strains from the Johnson-Cook constitutive model and the Zerilli-Armstrong model using several values of the temperature. The strain at necking predicted by the Johnson-Cook equation does not.vary with temperature and varies only slightly with strain rate. The strain at necking predicted by the modified Johnson-Cook model does not vary with temperature or strain rate. Figures 2 and 3 present the true stress at necking vs. the initial strain rate with temperature as a parameter for the Zerilli-Armstrong and Johnson-Cook models, respectively.

2.3 ΔV Equations. The ΔV between particulated jet particles is calculated based on the equation for the propagation of plastic deformation along a wire as reported by Kolsky (1963). This equation is used to determine the velocity at which a wire would break during the wire drawing fabrication process. This equation, as applied to a stretching shaped charge jet (Walters and Summers 1992), provides an expression for the velocity difference ΔV as

Figure 1. The Necking Strain as a Function of the Initial Strain Rate With Jet Temperature as a Parameter for the Zerilli-Armstrong and Johnson-Cook Constitutive Equation.

Figure 2. The Stress at Necking as a Function of the Initial Strain Rate With Jet Temperature as a Parameter for the Zerilli-Armstrong Constitutive Equation.

14
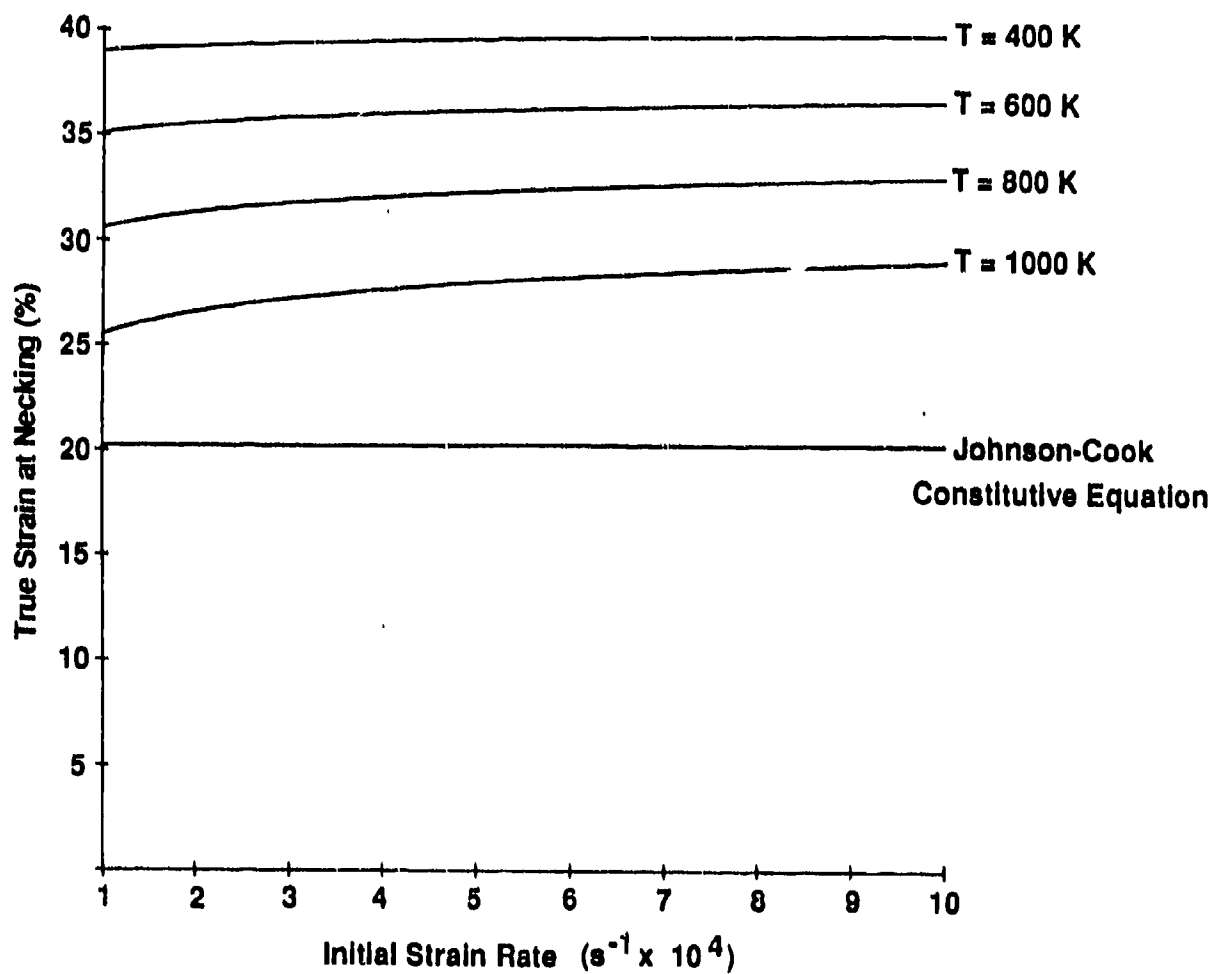
Figure 3. The Stress at Necking as a Function of the Initial Strain Rate With Jet Temperature as a Parameter for the Johnson-Cook Constitutive Equation.

$$\Delta V = \int_0^{\varepsilon_{e_N}} \sqrt{\frac{d\sigma_e/d\varepsilon_e}{\rho}} \ d\varepsilon_e , \qquad (6)$$

where ρ is the initial density of the jet, σ_e is the engineering stress, and ε_e is the engineering strain. The strain ε_{e_N} corresponds to the ultimate tensile strength of the jet, and the velocity corresponding to ε_{e_N} is the velocity at which the jet will break. This formula can be extended to account for a reduction in the cross-sectional area of the wire (or jet) (Walters and Summers 1992).

Based on the chosen constitutive equation, the velocity difference between particles can be calculated from Equation 1. This was accomplished in several ways. The constitutive equations and the plastic stability criterion are expressed in terms of true stresses and strains, and the ΔV equation is expressed in terms of engineering stresses and strains. One approach is to ignore the difference between true and engineering strains/stresses and combine the formulas directly (Walters and Summers 1992). With these assumptions (valid only for small strains), the best agreement with the experimental data is obtained. Table 3 depicts the results for this ΔV calculation and compares the calculations to the average experimental ΔV for several shaped charges with copper liners. The Zerilli-Armstrong constitutive equation was used with a temperature of 625 K. Also, the strain at necking was treated as an engineering strain.

In spite of the excellent agreement with the experimental data, this model was deemed inaccurate since the engineering and true strains are not exactly equal, as can be seen in Table 2. A more accurate, and rigorous, result may be obtained by working with either only true stresses and strains or with engineering stresses and strains. Converting Equation 6 to true stress and strain values yields

$$\Delta V = \frac{1}{\sqrt{\rho}} \int_0^{\varepsilon_{e_N}} \sqrt{\frac{d\sigma_e}{d\varepsilon_e}} \ d\varepsilon_e = \frac{1}{\sqrt{\rho}} \int_0^{\varepsilon_N} \sqrt{\frac{d\sigma}{d\varepsilon} - \sigma} \ d\varepsilon , \qquad (7)$$

Table 3. Analytical Calculation of the Average Velocity Difference Between Particles Assuming the True and Engineering Stresses/Strains Are Equivalent

Liner	ΔV (km/s) Experimental	ΔV (km/s) Analytical
81-mm cone	0.103–0.111	0.0993
65-mm cone	0.09–0.116	0.1014
101.6-mm cone	0.126	0.0989
163-mm trumpet	0.096–0.097	0.0966
76.2-mm hemisphere	0.097–0.100	0.0995

where the strain rate is allowed to vary with strain and the subscript N denotes the strain at necking. Calculations of ΔV were obtained from Equation 7 for both the Zerilli-Armstrong and Johnson-Cook constitutive models by numerical integration. In all cases, isothermal deformation was assumed, i.e., $T \neq T(\varepsilon)$.

However, numerical integration of Equation 7 is cumbersome when app"ed in conjunction with a jet formation code and provides little insight into the functional dep..dencies of ΔV on temperature, initial strain rate, etc. Equation 7 may be directly integrated under two assumptions. First, if $d\sigma/d\varepsilon$ is assumed to be much greater than σ (true for small strains), then

$$\Delta V = \frac{1}{\sqrt{\rho}} \int_0^{\varepsilon_N} \sqrt{\frac{d\sigma}{d\varepsilon}} \, d\varepsilon. \tag{8}$$

Second, if the strain rate is taken to be constant, i.e., $\dot{\varepsilon} = \dot{\varepsilon}_o$, then

$$\Delta V = \frac{4}{3} \varepsilon_N^{3/4} \sqrt{\frac{\dot{\varepsilon}_o^{C_4 T} C_2 \exp(-C_3 T)}{2\rho}} \tag{9}$$

17

using the Zerilli-Armstrong constitutive equation. For the Johnson-Cook model, Equation 8 (evaluated under the assumption of constant strain rate) yields

$$\Delta V = \frac{2}{n+1} \varepsilon_N^{\frac{n+1}{2}} \sqrt{\frac{(1 + C \ln \dot{\varepsilon}_o)(1 - T^{*m}) n B}{\rho}} \; . \tag{10}$$

Similarly, for the modified Johnson-Cook relation

$$\Delta V = \frac{2}{n+1} \varepsilon_N^{\frac{n+1}{2}} \sqrt{\frac{\dot{\varepsilon}_o^c (1 - T^{*m}) n B}{\rho}} \; . \tag{11}$$

If Equation 8 is evaluated for a variable strain rate or $\dot{\varepsilon} = \dot{\varepsilon}(\varepsilon)$, numerical integration is necessary. This was done for the Zerilli-Armstrong model with very little change in the calculated ΔV.

Finally, the most theoretically correct equation, Equation 7, was evaluated by approximate methods in order to develop a simple model to compete with the ΔV models listed in Table 1. The approximate solution was obtained by series expansion and term-by-term integration. The expansion is obtained from

$$\sqrt{\frac{d\sigma_e}{d\varepsilon_e}} = \frac{\exp(-\varepsilon)}{\sqrt{2} \; \varepsilon^{1/4}} \Big[C_2 \exp(-C_3 T) \dot{\varepsilon}^{C_4 T} - 2 C_1 \sqrt{\varepsilon}$$
$$- 2 C_2 \exp(-C_3 T) \dot{\varepsilon}^{C_4 T} (1 + C_4 T) \varepsilon \Big]^{1/2} \; ,$$

where $C_1 = C_o + \dfrac{k}{\sqrt{\lambda}}$ for the Zerilli-Armstrong constitutive equation. The term $\exp(-\varepsilon)$ is represented by a series expansion, and the square root term is expanded by the binomial theorem since

18

$$(C_2 \exp(-C_3 T) \, \dot{\varepsilon}^{C_4 T})^2 > 4 \, [C_1 \sqrt{\varepsilon} + C_2 \exp(-C_3 T) \, \dot{\varepsilon}^{C_4 T} (1 + C_4 T) \, \varepsilon]^2 \,.$$

If the series expansions are inserted into the integrand, multiplied together, and the result integrated term by term, the dominant term results in

$$\Delta V = \frac{4}{3} \, \varepsilon_N^{3/4} \sqrt{\frac{\dot{\varepsilon}^{C_4 T} \, C_2 \exp(-C_3 T)}{2\rho}} \,. \tag{12}$$

This expression is nearly identical to Equation 9 but allows for a variable strain rate. If ΔV is expressed in terms of the stress,

$$\Delta V = \frac{4}{3} \sqrt{\frac{\sigma - C_o - k/\sqrt{\lambda}}{2\rho}} \left[\frac{\sigma - C_o - k/\sqrt{\lambda}}{C_2 \exp(-C_3 T) \, \dot{\varepsilon}^{C_4 T}} \right] . \tag{13}$$

This expression, when compared to the results of other investigators, as shown in Table 1, shows the same dependence on $\rho^{-1/2}$ but varies as $(\sigma - C_1)^{3/2}$ instead of $\sqrt{\sigma}$. Equation 13 clearly shows the functional dependence of ΔV on the grain size of the liner. As expected, the velocity difference between particulated jet particles will decrease with decreasing grain size.

3. RESULTS

Table 4 lists the calculated strains, stresses, and average ΔV for each of these models. Basically, the Zerilli-Armstrong constitutive equation yields ΔV values in closer agreement with the experimental data than the Johnson-Cook based models. There is no significant difference in the values of ΔV calculated using either the Johnson-Cook or the modified Johnson-Cook relation. As before, the Zerilli-Armstrong grain size of 0.075 mm was used along with a temperature of 625 K. Equation 12 is chosen as our final ΔV formula since it is simple and agrees with the experimental data as well as any of the other models.

It is perhaps worthy of mention that Kennedy (1990) claimed that the ΔV between jet particles used in the breakup time model of Hirsch ranged from 0.055 km/s for a precision shaped charge to 0.18 km/s for a "crude" shaped charge. Also, Kennedy stated that ΔV decreases as the jet ductility increases. The ΔV of 0.055 km/s, is in close agreement with the ΔV calculations using Equation 7, which is theoretically the most accurate expression for ΔV.

19

Table 4. Calculated ΔV, ε_N, and σ_N Values for the Various Models Used In This Study

		Warhead				
	Const. Eqn.	65 mm Cone	101.6 mm Cone	81 mm Cone	163 mm Trumpet	76.2 mm Hemisphere
ΔV_7 (km/s)[a]	Z-A[c]	0.061	0.060	0.060	0.058	0.060
ΔV_7 (km/s)	J-C[d]	0.039	0.039	0.039	0.038	0.039
ΔV_7 (km/s)	M J-C[e]	0.039	0.039	0.039	0.039	0.039
ΔV_8 (km/s)	Z-A	0.087	0.085	0.085	0.083	0.085
ΔV_9 (km/s)	Z-A	0.087	0.085	0.086	0.083	0.086
ΔV_{10} (km/s)	J-C	0.052	0.052	0.052	0.051	0.052
ΔV_{11} (km/s)	M J-C	0.053	0.052	0.052	0.052	0.052
ΔV_{12} (km/s)	Z-A	0.086	0.084	0.085	0.082	0.085
ΔV_{exp} (km/s)	—	0.107	0.126	0.108	0.097	0.099
ε_N[b]	Z-A	0.361	0.358	0.359	0.355	0.359
σ_N (MPa)	Z-A	271.9	264.1	265.6	257.2	266.1
ε_N	J-C	0.202	0.202	0.202	0.202	0.202
σ_N (MPa)	J-C	246.7	244.4	244.8	242.3	245.0
ε_N	M J-C	0.201	0.201	0.201	0.201	0.201
σ_N (MPa)	M J-C	254.9	251.9	252.4	249.1	252.6

[a] The subscript on ΔV represents the equation number
[b] The subscript N denotes stress or strain values at necking
[c] Z-A denotes Zerilli-Armstrong
[d] J-C denotes Johnson-Cook
[e] M J-C denotes modified Johnson-Cook

If the necking strain from the Zerilli-Armstrong model is taken as 0.360 for all the copper liners used in this study, then for cylindrical jet particles

$$\exp(-\varepsilon_N) = \frac{A}{A_o} = \frac{r^2}{r_o^2},$$

or the radius of the jet at the necking strain would be $r = 0.835\ r_o$. This would indicate that this strain is closer to the actual data than the Johnson-Cook strain calculation although experimental data regarding the jet radius just prior to particulation is scarce. The stress values predicted by either constitutive model are in the range of 100–300 MPa as quoted by other investigators. The predicted ΔV values are lower than the average experimental values by about 20%. The ΔV values predicted by the current study show a variation with the liner geometry due to the dependence of ΔV on the strain rate. The previous models predict the same ΔV for all charges with the same liner material, since ΔV depends only on the stress.

The experimentally determined ΔV is shown in Figure 4 for the 81-mm copper conical liner shaped charge. Note that the ΔV values, measured for each jet particle, range from nearly 0 to 0.250 km/s. It is amazing in view of the scatter of the ΔV data that the average ΔV is usually 0.11 km/s (depicted by the dashed line on Figure 1) for shaped charges with 42° copper conical liners. The solid curve on Figure 4 shows the incremental ΔV calculations obtained by using Equation 9 in conjunction with a jet formation code. The jet temperature was assumed to be 625 K and constant throughout the jet. The copper grain size was taken to be 0.075 mm. The "hook" in the analytical curve near the tip region is due to the change in jet velocity between liner elements being nearly zero for elements near the tip due to the inverse velocity gradient and the tip formation process. Note that the current theory falls well within the range of experimental data.

Also, the current model is dependent on the jet temperature used in the Zerilli-Armstrong constitutive equation. Tables 5–10 present the calculated ΔV values and the stress and strain values at necking as a function of temperature for several shaped charges with copper liners. Table 5 is for a 81-mm diameter shaped charge with a copper conical liner. This table presents several of the ΔV models discussed earlier for various temperatures. The remainder of the tables present one ΔV calculation (Equation 9), but the stress and strain values at necking are given for both constitutive equation models.

For all the cases studied, a very close match to the experimental data can be obtained if the jet temperature is assumed to be lower than the average values quoted by von Holle and Trimble.
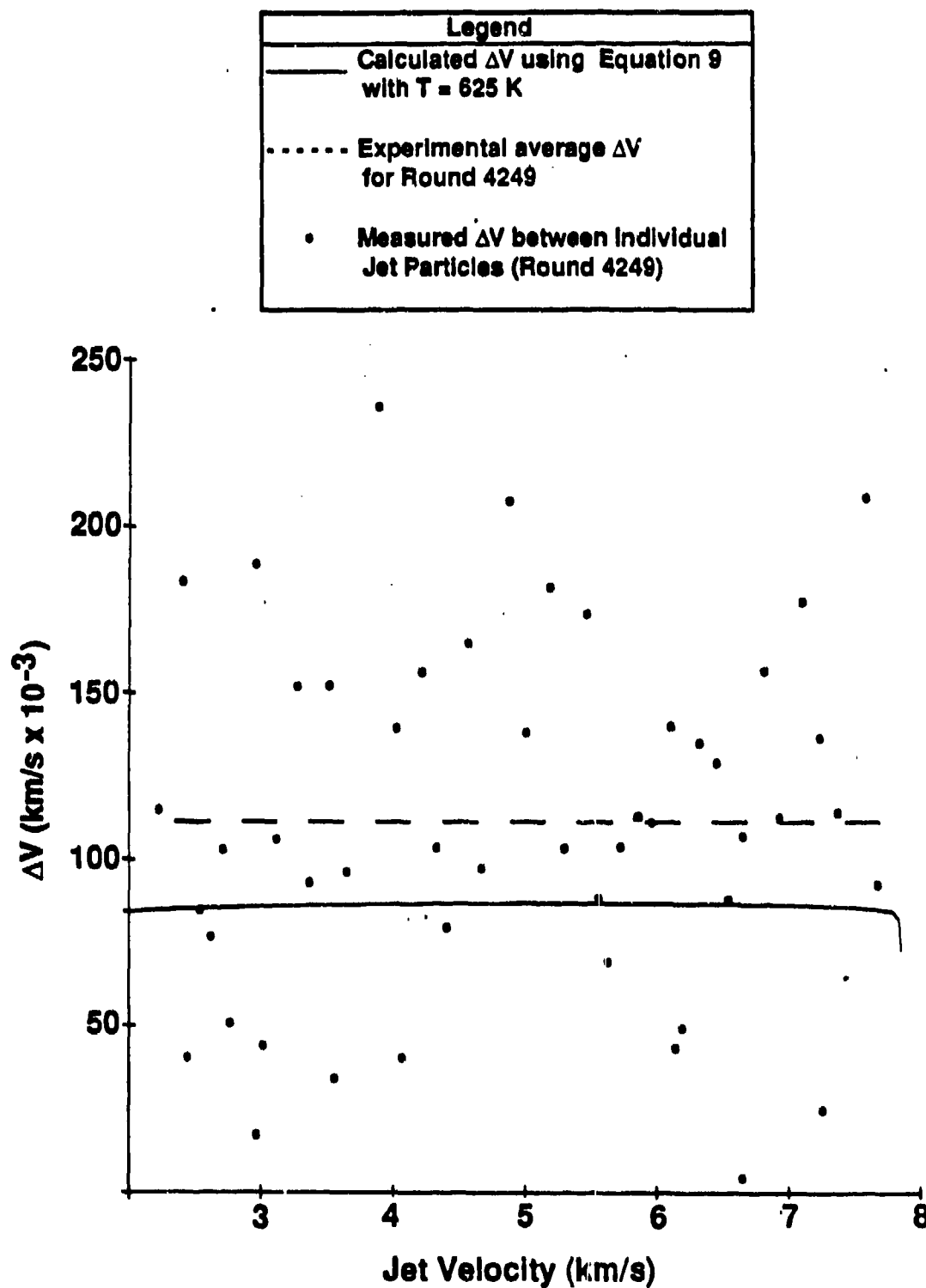
Figure 4. Analytical and Experimental Values for the Velocity Difference Between Particles During the Jet Formation Process for the 81-mm Conical Copper Liner.

Table 5. The Average Velocity Difference Between Particles for Several Analytical Models and the Stress and Strain Values at Necking With Temperature as a Paramenter for the 81-mm Cone

Liner: 81-mm cone
Explosive fill: Composition B
Initial strain rate: 67,957 s^{-1}
Measured ΔV values (round number): 0.110 (4248), 0.111 (4249), 0.107 (4250), 0.111 (4251), 0.103 (4252)

Temperature (K)	ΔV (km/s)				
	Eq. 7 $_{Z-A}$[a]	Eq. 7 $_{J-C}$[b]	Eq. 9 $_{Z-A}$	Eq. 10 $_{J-C}$	Eq. 11 $_{Z-A}$
400	0.0772	0.0436	0.1095	0.0583	0.1085
500	0.0691	0.0415	0.0984	0.0555	0.0973
600	0.0615	0.0392	0.0881	0.0524	0.0870
700	0.0546	0.0366	0.0785	0.0490	0.0775
800	0.0482	0.0339	0.0697	0.0453	0.0687
900	0.0422	0.0308	0.0616	0.0411	0.0606
1,000	0.0368	0.0273	0.0541	0.0365	0.0532
Temperature (K)	ε_{Z-A}	σ_{Z-A} (MPa)	ε_{J-C}	σ_{J-C} (MPa)	
400	0.396	364.2	0.202	312.8	
500	0.380	315.8	0.202	283.4	
600	0.363	274.8	0.202	252.7	
700	0.345	240.1	0.202	221.0	
800	0.326	210.8	0.202	188.7	
900	0.305	186.0	0.202	155.7	
1,000	0.284	165.1	0.202	122.2	

[a] Z-A denotes Zerilli-Armstrong
[b] J-C denotes Johnson-Cook

Table 6. Analytical ΔV Values From Equation 9 and the Stress and Strain Values at Necking With Temperature as a Parameter for the 65-mm Cone

Liner: 65-mm cone
Explosive fill: LX-14
Initial strain rate: 99,909 s^{-1}
Measured ΔV values (round number): 0.09 (3813), 0.115 (4253), 0.116 (4254)

Temperature (K)	ΔV (km/s)	E_{Z-A}[a]	σ_{Z-A} (MPa)	ε_{J-C}[b]	σ_{J-C} (MPa)
400	0.1107	0.397	370.0	0.202	315.1
500	0.0998	0.382	322.0	0.202	285.6
600	0.0897	0.365	281.1	0.202	254.6
700	0.0803	0.348	246.4	0.202	222.7
800	0.0716	0.329	216.9	0.202	190.1
900	0.0635	0.310	191.9	0.202	156.9
1,000	0.0561	0.290	170.6	0.202	123.2

[a] Z-A denotes Zerilli-Armstrong
[b] J-C denotes Johnson-Cook

Table 7. Analytical ΔV Values From Equation 9 and the Stress and Strain Values at Necking With Temperature as a Parameter for the 76.2-mm Hemisphere

Liner: 76.2 mm hemisphere
Explosive fill: 75/25 OCTOL
Initial strain rate: 70,179 s^{-1}
Measured ΔV values (round number): 0.097 (4066), 0.100 (4135)

Temperature (K)	ΔV (km/s)	ε_{Z-A}[a]	σ_{Z-A} (MPa)	ε_{J-C}[b]	σ_{J-C} (MPa)
400	0.1096	0.396	364.6	0.202	313.0
500	0.0985	0.380	316.3	0.202	283.6
600	0.0882	0.363	275.3	0.202	252.8
700	0.0787	0.345	240.6	0.202	221.2
800	0.0699	0.326	211.3	0.202	188.8
900	0.0617	0.306	186.5	0.202	155.8
1,000	0.0542	0.285	165.6	0.202	122.3

[a] Z-A denotes Zerilli-Armstrong
[b] J-C denotes Johnson-Cook

Table 8. Analytical ΔV Values From Equation 9 and the Stress and Strain Values at Necking With Temperature as a Parameter for the 101.6-mm Cone

Liner: 101.6 mm Cone
Explosive fill: 75/25 OCTOL
Initial strain rate: 62,221 s^{-1}
Measured ΔV values (round number): 0.126 (4038)

Temperature (K)	ΔV (km/s)	ε_{Z-A}[a]	σ_{Z-A} (MPa)	ε_{J-C}[b]	σ_{J-C} (MPa)
400	0.1092	0.396	362.8	0.202	312.2
500	0.0980	0.380	314.4	0.202	282.9
600	0.0877	0.362	273.4	0.202	252.2
700	0.0781	0.344	238.7	0.202	220.6
800	0.0693	0.325	209.4	0.202	188.3
900	0.0611	0.304	184.7	0.202	155.4
1,000	0.0536	0.283	163.9	0.202	122.0

[a] Z-A denotes Zerilli-Armstrong
[b] J-C denotes Johnson-Cook

Table 9. Analytical ΔV Values From Equation 9 and the Stress and Strain Values at Necking With Temperature as a Parameter for the 140-mm Cone

Liner: 140-mm cone
Explosive fill: 75/25 OCTOL
Initial strain rate: 43004 s^{-1}
Measured ΔV values (round number): 0.102 (4263), 0.096 (4264)

Temperature (K)	ΔV (km/s)	ε_{Z-A}[a]	σ_{Z-A} (MPa)	ε_{J-C}[b]	σ_{J-C} (MPa)
400	0.1080	0.395	357.4	0.202	309.9
500	0.0967	0.378	308.6	0.202	280.8
600	0.0862	0.360	267.5	0.202	250.4
700	0.0765	0.341	232.9	0.202	219.0
800	0.0675	0.321	203.8	0.202	187.0
900	0.0593	0.300	179.4	0.202	159.3
1,000	0.0517	0.277	158.9	0.202	121.1

[a] Z-A denotes Zerilli-Armstrong
[b] J-C denotes Johnson-Cook

Table 10. Analytical ΔV Values From Equation 9 and the Stress and Strain Values at Necking With Temperature as a Parameter for the 163-mm Trumpet

Liner: 163-mm trumpet
Explosive fill: LX-14
Initial strain rate: 40138 s⁻¹
Measured ΔV values (round number): 0.097 (4241), 0.096 (4242)

Temperature (K)	ΔV (km/s)	E $_{Z-A}$ [a]	σ $_{Z-A}$ (MPa)	ε $_{J-C}$ [b]	σ $_{J-C}$ (MPa)
400	0.1078	0.394	356.4	0.202	309.5
500	0.0964	0.378	307.5	0.202	280.5
600	0.0859	0.360	266.4	0.202	250.1
700	0.0762	0.341	231.9	0.202	218.7
800	0.0672	0.320	202.8	0.202	186.7
900	0.0590	0.299	178.4	0.202	154.1
1,000	0.0514	0.276	158.0	0.202	121.0

[a] Z-A denotes Zerilli-Armstrong
[b] J-C denotes Johnson-Cook

Namely, a temperature of 400–500 K will yield a ΔV in complete agreement with the jet experimental data. Of course, the jet temperature obviously varies through the jet and along the jet from tip to tail. Also, von Holle and Trimble report considerable scatter in their temperature data. All theoretical calculations of jet temperature (by Pfeffer and Racah, see Walters 1991), predict temperatures at the low end of the measured values, i.e., about 450–500 K. Also, Robinson (1957) concluded that the jet temperature must be lower than 500 K, or that insufficient heat transfer occurs between the jet and the target. These conclusions were based on copper jets fired into paper and other materials with self-ignition temperatures of 450–500 K. In short, the distribution of jet temperature as required for our ΔV model is simply not known. In Tables 5–10, the explosive fill is given since the von Holle-Trimble jet temperature measurements show a jet temperature variation with the explosive fill. However, a trend regarding ΔV with explosive fill was not apparent from the current study.

The tabulated data is plotted in Figures 5–7. Figure 5 shows the ΔV calculated from Equation 9 with the Zerilli-Armstrong constitutive equation vs. initial strain rate for several values of the temperature. The experimental points for the six copper rounds used in this study are also shown on Figures 5–7. Figure 6 is a similar plot for the Johnson-Cook
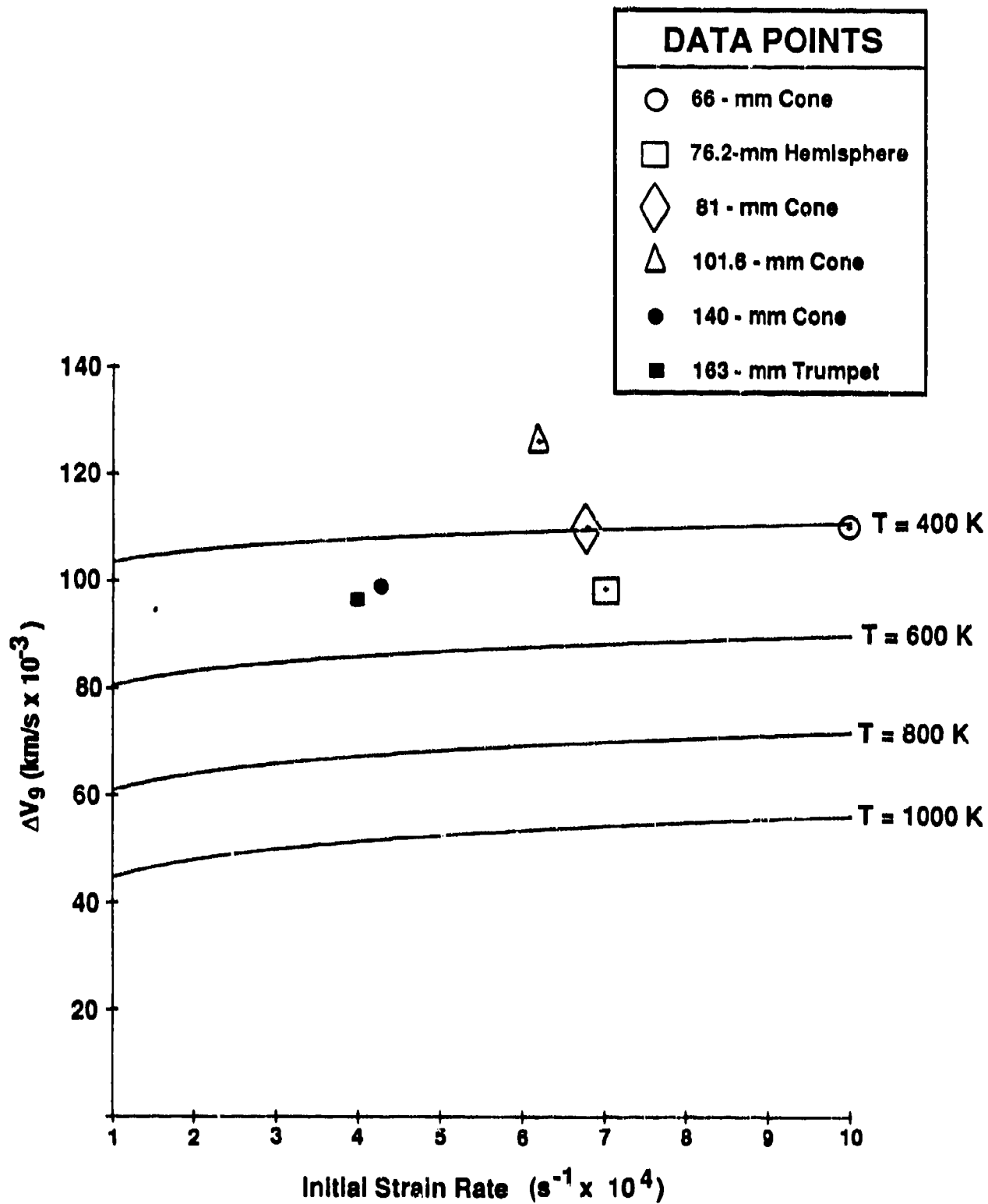
Figure 5. The Calculated ΔV, Based on Equation 9, as a Function of the Initial Strain Rate With Jet Temperature as a Parameter.
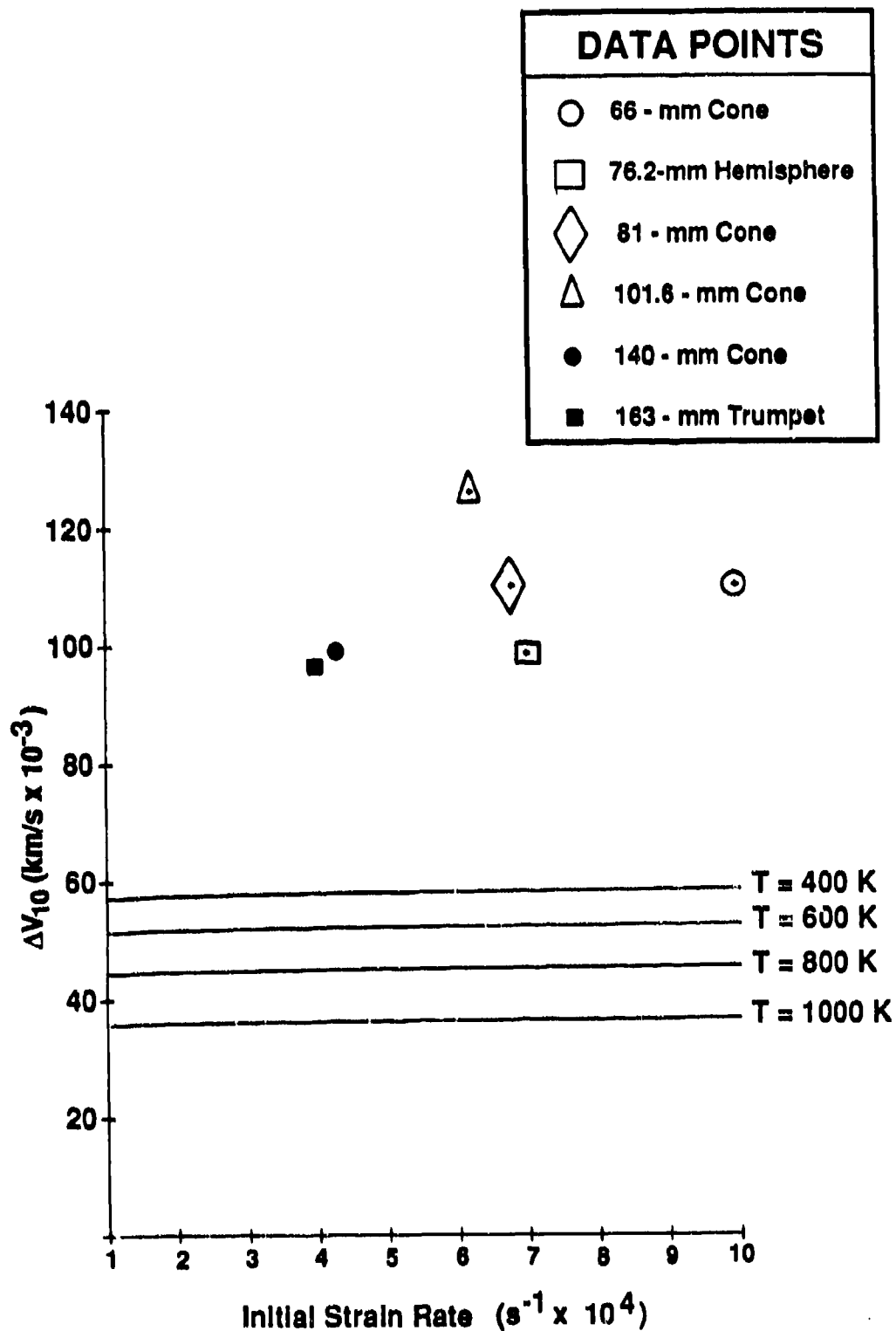
Figure 6. The Calculated ΔV, Based on Equation 10, as a Function of the Initial Strain Rate With Jet Temperature as a Parameter.
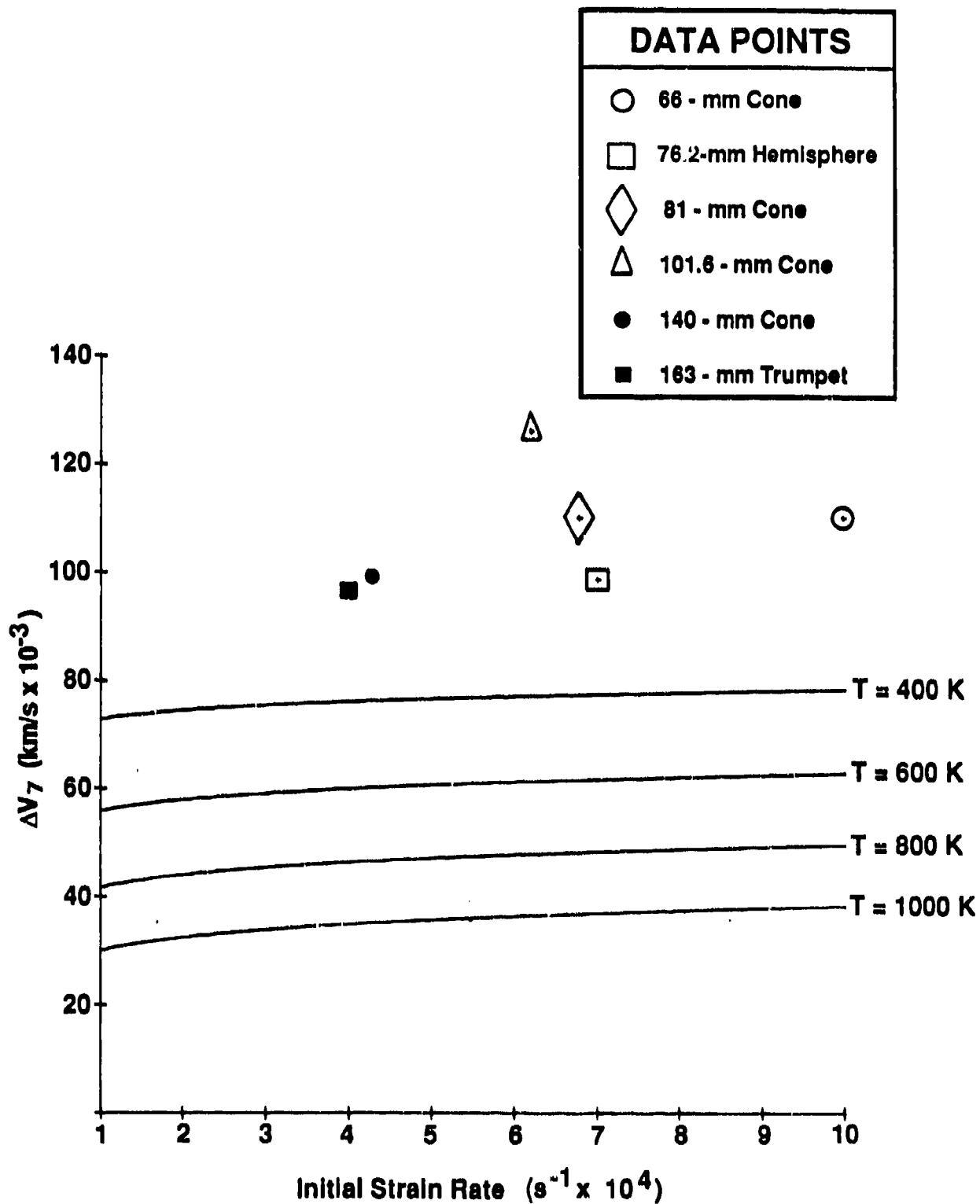
Figure 7. The Calculated ΔV, Based on Equation 7, as a Function of the Initial Strain Rate With Jet Temperature as a Parameter for the Zerilli-Armstrong Relationship.

relationship with ΔV from Equation 10. Figure 7 is based on Zerilli-Armstrong and ΔV from Equation 7. Note that the initial strain rate has only a small effect on ΔV. The temperature has a much larger effect. Figure 6 illustrates the lower predictions using the Johnson-Cook model for all temperatures.

4. CONCLUSIONS

A model was derived to predict the ΔV between particulated jet particles. The model was derived from the "wire drawing" equation reported by Kolsky, the criterion for plastic instability, and an appropriate constitutive equation. The calculated results were well within the range of the experimental data for the six different copper shaped charges we studied. However, the calculated average ΔV value was below the experimental average.

The model allows for variation in initial strain rate and can thus distinguish between different liner designs, unlike other models. The ΔV calculations are also dependent on temperature and may be more accurate than indicated once accurate calculations or experiments are conducted to determine the jet temperature gradients. The model is valid for any face-centered-cubic material, and the Zerilli-Armstrong constitutive equation was deemed to be superior to the Johnson-Cook equation for studies of this nature. Copper was the only face-centered-cubic material considered in this study because we lacked either a known constitutive equation or sufficient experimental data for other face-centered-cubic liner materials.

5. REFERENCES

Chokshi, A. H., and M. A. Meyers. "The Prospects for Superplasticity at High Strain Rates: Preliminary Considerations and an Example." Scripta Metallurgical et Materialia, vol. 24, pp. 605–610, 1990.

Chou, P. C., and J. Carleone. "The Breakup of Shaped Charge Jets." Proceedings of the Second International Symposium on Ballistics, Daytona Beach, FL, March 1976.

Chou, P. C., and J. Carleone. "The Stability of Shaped Charge Jets." Journal of Applied Physics, vol. 48, no. 10, pp. 4187–4195, October 1977a.

Chou, P. C., and J. Carleone. "The Stability and Breakup of Shaped Charge Jets." Third International Symposium on Ballistics, Karlsruhe, Germany, March 1977b.

Chou, P. C., J. Carleone, and R. R. Karpp. "Study of Shaped Charge Jet Formation and Breakup." BRL-CR-138, U.S. Army Ballistic Research Laboratory, Aberdeen Proving Ground, MD, February 1974.

Chou, P. C., and W. J. Flis. "Recent Developments in Shaped Charge Technology." Propellants, Explosives, and Pyrotechnics, vol. 11, pp. 99–114, 1986.

Chou, P. C., H. S. Sidhu, and R. W. Mortimer. "A Study of the Break-Up of Shaped Charge Jets." DIT Report No. 125-4, Drexel University, Philadelphia, PA, April 1963.

Golaski, S. K., and M. L. Duffy. "Effect of Liner Grain Size on Shaped Charge Jet Performance and Characteristics." BRL-TR-2800, U.S. Army Ballistic Research Laboratory, Aberdeen Proving Ground, MD, April 1987.

Haugstad, B. "On the Break-Up of Shaped Charge Jets." Propellants, Explosives, and Pyrotechnics, vol. 8, pp. 119–120, 1983.

Haugstad, B., and O. Dullum. "The Jet Fragmentation Problem and Its Relation to Shaped Charge Engineering." Unpublished paper presented at MBB, Schrobenhausen, Germany, September 1983.

Held, M. "Determination of the Material Quality of Copper Shaped Charge Liners." Propellants, Explosives, and Pyrotechnics, vol. 10, pp. 125–128, 1985.

Held, M. "Particulation of Shaped Charge Jets." Proceedings of the Eleventh International Symposium on Ballistics, Brussels, May 1989.

Hirsch, E. "A Formula for the Shaped Charge Jet Break-Up Time." Propellants and Explosives, vol. 4, pp. 89–94, 1979.

Hirsch, E. "A Model Explaining the Rule for Calculating the Break-Up Time of Homogeneous Ductile Metals." Propellants and Explosives, vol. 6, pp. 11–14, 1981a.

Hirsch, E. "The Natural Spread and Tumbling of the Shaped Charge Jet Segments."
Propellants and Explosives, vol. 6, pp. 104–111, 1981b.

Hirsch, E. "The Effect of the Liner Metallurgical State on the Shaped Charge Jet Break-Up
Time." Propellants, Explosives, and Pyrotechnics, vol. 15, pp. 166–176, 1990.

Hirsch, E. "Internal Shearing During Shaped Charge Jet Formation and Break-Up."
Propellants, Explosives, and Pyrotechnics, vol. 17, pp. 27–33, 1992.

Johnson, G. R. "Development of Strength and Fracture Models for Computations Involving
Severe Dynamic Loading Volume 1: Strength and Fracture Models." AFATL-TR-83-05, Air
Force Armament Laboratory, Eglin AFB, FL, January 1983.

Johnson, G. R., and W. H. Cook. Proceedings of the Seventh International Symposium on
Ballistics. The Hague, The Netherlands, p. 541, 1983.

Johnson, G. R., and W. H. Cook. "Fracture Characteristics of Three Metals Subjected to
Various Strains, Strain Rates, Temperatures and Pressures." Engineering Fracture
Mechanics, vol. 21, no. 1, pp. 31–48, 1985.

Kennedy, D. R. "The Design of Multi-Staged Shaped Charges Using the "BRIGS" Analytical
Computer Model." Proc. of the 12th International Ballistics Symposium, San Antonio, TX,
1990.

Kolsky, H. Stress Waves in Solids. Chapter 7, New York: Dover, 1963.

Mostert, F. J., and P. J. Koenig. "A Link Between Liner Metallurgy and Shaped Charge Jet
Ductility." South African Journal of Physics, vol. 10, no. 3, 1987.

Pfeffer, G. "Determination Par Simulations Numeriques De L'etat et Des Lois De
Fragmentation Des Jets De Charges Crueses." Proceedings of the Fifth International
Symposium on Ballistics, Toulouse, France, April 1980.

Robinson, R. L. "Temperature Effect on Formation During Jet Perforating." Journal of
Petroleum Technology. Vol. 9, 1957.

Shelton, R. D., and A. L. Arbuckle. "A Calculation of Particle Size Distributions in the Breakup
of Shaped Charge Jets." Journal of Applied Physics, vol. 50, no. 10, October 1979.

Summers, R. L., and K. C. Wright. "The Experimental Assessment of Jet Transverse
Velocty." Development in Theoretical and Applied Mechanics, vol. 16. Edited by B. Antar,
R. Engels, A. A. Prinaris, and T. H. Moulden, University of Tennessee Space Institute,
1992.

Walsh, J. M. "Plastic Instability and Particulation in Stretching Metal Jets." Journal of Applied
Physics, vol. 56, no. 7, October 1984.

Walters, W. P. "Shock Waves in the Study of Shaped Charges." BRL-TR-3258, U.S. Army
Ballistic Research Laboratory, Aberdeen Proving Ground, MD, August 1991.

Walters, W. P., and R. L. Summers. "The Particulation of a Shaped Charge Jet." <u>Development in Theoretical and Applied Mechanics</u>, vol. 16, edited by B. Antar, R. Engels, A. A. Prinaris, and T. H. Moulden, University of Tennessee Space Institute, 1992.

Walters, W. P., and J. A. Zukas. <u>Fundamentals of Shaped Charges</u>. New York: John Wiley and Sons, 1989.

Zerilli, F., and R. Armstrong. "Dislocation-Mechanics-Based Constitutive Relations for Material Dynamics Calculations." <u>Journal of Applied Physics</u>, vol. 61 (5), pp. 1816–1825, March 1987.

INTENTIONALLY LEFT BLANK.

No. of
Copies Organization

2   Administrator
Defense Technical Info Center
ATTN: DTIC-DDA
Cameron Station
Alexandria, VA 22304-6145

1   Commander
U.S. Army Materiel Command
ATTN: AMCAM
5001 Eisenhower Ave.
Alexandria, VA 22333-0001

1   Director
U.S. Army Research Laboratory
ATTN: AMSRL-D
2800 Powder Mill Rd.
Adelphi, MD 20783-1145

1   Director
U.S. Army Research Laboratory
ATTN: AMSRL-OP-CI-A,
        Tech Publishing
2800 Powder Mill Rd.
Adelphi, MD 20783-1145

2   Commander
U.S. Army Armament Research,
   Development, and Engineering Center
ATTN: SMCAR-IMI-I
Picatinny Arsenal, NJ 07806-5000

2   Commander
U.S. Army Armament Research,
   Development, and Engineering Center
ATTN: SMCAR-TDC
Picatinny Arsenal, NJ 07806-5000

1   Director
Benet Weapons Laboratory
U.S. Army Armament Research,
   Development, and Engineering Center
ATTN: SMCAR-CCB-TL
Watervliet, NY 12189-4050

(Unclass. only)1   Commander
U.S. Army Rock Island Arsenal
ATTN: SMCRI-TL/Technical Library
Rock Island, IL 61299-5000

1   Director
U.S. Army Aviation Research
   and Technology Activity
ATTN: SAVRT-R (Library)
M/S 219-3
Ames Research Center
Moffett Field, CA 94035-1000

No. of
Copies Organization

1   Commander
U.S. Army Missile Command
ATTN: AMSMI-RD-CS-R (DOC)
Redstone Arsenal, AL 35898-5010

1   Commander
U.S. Army Tank-Automotive Command
ATTN: ASQNC-TAC-DIT (Technical
        Information Center)
Warren, MI 48397-5000

1   Director
U.S. Army TRADOC Analysis Command
ATTN: ATRC-WSR
White Sands Missile Range, NM 88002-5502

1   Commandant
U.S. Army Field Artillery School
ATTN: ATSF-CSI
Ft. Sill, OK 73503-5000

(Class. only)1   Commandant
U.S. Army Infantry School
ATTN: ATSH-CD (Security Mgr.)
Fort Benning, GA 31905-5660

(Unclass. only)1   Commandant
U.S. Army Infantry School
ATTN: ATSH-CD-CSO-OR
Fort Benning, GA 31905-5660

1   WL/MNOI
Eglin AFB, FL 32542-5000

Aberdeen Proving Ground

2   Dir, USAMSAA
ATTN: AMXSY-D
      AMXSY-MP, H. Cohen

1   Cdr, USATECOM
ATTN: AMSTE-TC

1   Dir, ERDEC
ATTN: SCBRD-RT

1   Cdr, CBDA
ATTN: AMSCB-CI

1   Dir, USARL
ATTN: AMSRL-SL-I

10   Dir, USARL
ATTN: AMSRL-OP-CI-B (Tech Lib)

6   Commander
Naval Surface Warfare Center
ATTN: Code DG-50,
      W. Reed, R10A
      E. Johnson
      W. Bullock
      F. Zerilli
      R. Garrett
White Oak, MD 20910

2   Commander
U.S. Army Armament Research,
   Development, and Engineering Center
ATTN: SMCAR-AWE,
      J. Pearson
      J. Grant
Picatinny Arsenal, NY 07806-5000

3   Director
DARPA
ATTN: J. Richardson
      LTC Quinn
      T. Hafer
3701 North Fairfax Dr.
Arlington, VA 22203-1714

3   Commander
U.S. Army Missile Command
ATTN: AMSMI-RD-ST-WF,
      M. Schexnayder
      S. Cornelius
      S. Hill
Redstone Arsenal, AL 35898-5247

1   AFATL/DLJR
ATTN: J. Foster
Eglin AFB, FL 32542

1   WRDC/MTX
ATTN: Mr. Lee Kennard
Wright Patterson AFB, OH 45433-6533

1   U.S. Army Harry Diamond Laboratories
ATTN: SLCHD-TA-SS,
      Bob Christopherson
2800 Powder Mill Road
Adelphi, MD 20783-1197

5   Director
Lawrence Livermore Laboratory
ATTN: Technical Library
      Dr. J. Kury
      Dr. M. Van Thiel
      Dr. C. Cline
      Dr. D. Bauman
P.O. Box 808
Livermore, CA 94550

3   Battelle
ATTN:TACTEC Library, J.N. Huggins
      Dr. L. Vescilius
      Dr. B. Dale Trott
505 King Avenue
Columbus, OH 43201

3   Director
Sandia National Laboratories
ATTN: Dr. M. Forrestal
      Dr. M. Vigil
      Dr. A. Robinson
P.O. Box 5800
Albuquerque, NM 87185

7   University of California
Los Alamos Scientific Lab
ATTN: Dr. J. Walsh
      Dr. R. Karpp
      Dr. C. Mautz
      L. Hull, M-8
      J. Repa
      D. Fradkin
      Technical Laboratory
P.O. Box 1663
Los Alamos, NM 87545

1   Southwest Research Institute
ATTN: C. Anderson
P.O. Drawer 28255
San Antonio, TX 78284

1   Naval Ordnance Station
ATTN: B. Barger-Tyo, Code 6310C
Indian Head, MD 20640-5000

2   Battelle
    Edgewood Operations
    ATTN: R. Jameson
            S. Golaski
    2113 Emmorton Park Road
    Suite 200
    Edgewood, MD 21040

1   E.I. DuPont De Nemours & Company
    ATTN: B. Scott
    Chestnut Run - CR 702
    Wilmington, DE 19898

1   Dyna East Corporation
    ATTN: P.C. Chou
    3201 Arch Street
    Philadelphia, PA 19104

1   Aerojet Electro Systems Company
    ATTN: Warhead Systems,
            Dr. J. Carleone
    1100 W. Hollyvale St.
    P.O. Box 296
    Azusa, CA 91702

1   Physics International Company
    Tactical Systems Group
    Eastern Division
    P.O. Box 1004
    Wadsworth, OH 44281-0904

2   Alliant Techsystems, Inc.
    Marine Systems Group
    ATTN: G. Johnson
            J. Houlton
    600 Second Street, NE
    Hopkins, NM 55343

1   Nuclear Metals, Inc.
    ATTN: M. Waltz
    2229 Main Street
    Concord, MA 01742

1   Shock Transients, Inc.
    ATTN: David Davison, President
    P.O. Box 5357
    Hopkins, MN 55343

1   Physics International Company
    ATTN: R. Coffenbery
    P.O. Box 5010
    San Leandro, CA 94577-0599

1   S-Cubed
    ATTN: Dr. R. Sedgwick
    P.O. Box 1620
    La Jolla, CA 92038-1620

1   SRI International
    ATTN: Dr. L. Seaman
    333 Ravenswood Avenue
    Menlo Park, CA 94025

2   College of Engineering
    ATTN: Dr. R. D. Dick
            Dr. R. Armstrong
    College Park, MD 20742

1   University of Alabama
    Department of Engineering Mechanics
    ATTN: Dr. S. E. Jones
    P.O. Box 870278
    Tuscalosa, AL 35487-0278

1   California Research and Technology, Inc.
    ATTN: Mark Majerus
    50 Washington Road
    P.O. Box 2229
    Princeton, NJ 08543

INTENTIONALLY LEFT BLANK.

USER EVALUATION SHEET/CHANGE OF ADDRESS

This Laboratory undertakes a continuing effort to improve the quality of the reports it publishes. Your comments/answers to the items/questions below will aid us in our efforts.

1. ARL Report Number __ARL-TR-8__ _____ Date of Report __November 1992__

2. Date Report Received _____

3. Does this report satisfy a need? (Comment on purpose, related project, or other area of interest for which the report will be used.) _____

_____

_____

4. Specifically, how is the report being used? (Information source, design data, procedure, source of ideas, etc.)_____

_____

_____

5. Has the information in this report led to any quantitative savings as far as man-hours or dollars saved, operating costs avoided, or efficiencies achieved, etc? If so, please elaborate. _____

_____

_____

6. General Comments. What do you think should be changed to improve future reports? (Indicate changes to organization, technical content, format, etc.) _____

_____

_____

_____

CURRENT
ADDRESS

_____
Organization

_____
Name

_____
Street or P.O. Box No.

_____
City, State, Zip Code

7. If indicating a Change of Address or Address Correction, please provide the Current or Correct address above and the Old or Incorrect address below.

OLD
ADDRESS

_____
Organization

_____
Name

_____
Street or P.O. Box No.

_____
City, State, Zip Code

(Remove this sheet, fold as indicated, staple or tape closed, and mail.)